

Chapter 9

Laser Ablation Electrospray Ionization for Atmospheric Pressure Molecular Imaging Mass Spectrometry

Peter Nemes and Akos Vertes

Abstract

Laser ablation electrospray ionization (LAESI) is a novel method for the direct imaging of biological tissues by mass spectrometry. By performing ionization in the ambient environment, this technique enables *in vivo* studies with potential for single-cell analysis. A unique aspect of LAESI mass spectrometric imaging (MSI) is depth profiling that, in combination with lateral imaging, permits 3D molecular imaging for the first time under native conditions. With current lateral and depth resolutions of ~ 100 and ~ 40 μm , respectively, LAESI MSI helps to explore the molecular architecture of live tissues.

Key words: Mass spectrometry, imaging, ambient, direct analysis, depth profiling, three-dimensional, *in vivo*, tissue imaging.

1. Introduction

Traditional mass spectrometric imaging (MSI) methods, such as matrix-assisted laser desorption ionization (MALDI) and secondary ion mass spectrometry (SIMS), have become important tools for the investigation of molecular distributions in tissues due to their high ionization efficiencies and excellent lateral and depth resolutions. Invasive sample preparation and the need for vacuum conditions, however, are incompatible with the analysis of live samples.

Novel ionization methods in ambient mass spectrometry (1) overcome these limitations by performing imaging under native conditions. Desorption electrospray ionization (2), atmospheric pressure (AP) mid-infrared (mid-IR) MALDI (3), laser ablation

electrospray ionization (LAESI) (4), and most recently laser ablation coupled to flowing AP afterglow MS (5) have demonstrated imaging capabilities with lateral resolutions 20–400 μm while obtaining low limits of detection. **Figure 9.1a** shows the schematics of the LAESI ion source. **Figure 9.1b** depicts the fast imaging of the entrainment of laser-ablated particulates into the electro-spray plume. The interaction of the sprayed droplets with the particulates and neutrals emerging from the laser ablation (LA) produces coalesced charged particles that are thought to be the basis of the LAESI signal. In this chapter, we describe the protocols for lateral and 3D MSI of biological tissues using LAESI.

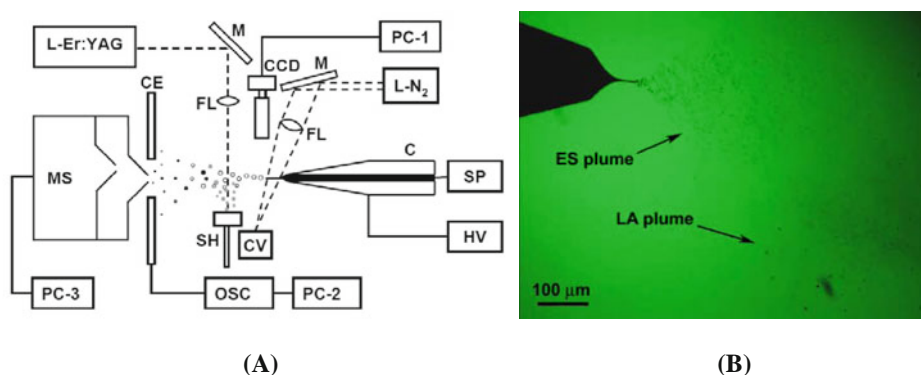


Fig. 9.1. (a) Schematics of the LAESI setup with (optional) spray current measurement and fast imaging system (C, capillary emitter; SP, syringe pump; HV, high-voltage power supply; L-N₂, nitrogen laser; M, mirrors; FL, focusing lenses; CV, cuvette; CE, counter electrode; OSC, digital oscilloscope; SH, sample holder; L-Er:YAG, Er:YAG laser; MS, mass spectrometer; PC-1 to PC-3, personal computers). *Open black dots* represent the droplets formed by the electro-spray. Their interaction with the particulates and neutrals (*solid gray dots*) emerging from the laser ablation produces some fused particles (*solid black dots*) that are thought to be the basis of the LAESI signal. (Adapted with permission from (6). Copyright 2007 American Chemical Society.) (b) Our fast imaging experiments supported this scenario. The image captured with ~ 10 ns exposure time shows the interaction of the laser ablation plume (LA) and the electro-spray plume (ES). (Adapted with permission from (6). Copyright 2007 American Chemical Society.)

2. Materials

2.1. Reagents and Sample

1. Electro-spray solution for positive ion mode analysis: 50% methanol or acetonitrile, 1% acetic acid or formic acid in water. **▼CAUTION:** Glacial acetic acid is extremely harmful when inhaled; causes burns to the skin and eyes; and avoid contact with skin, eyes, and the respiratory system.
2. Electro-spray solution for negative ion mode analysis: 50% methanol or acetonitrile, 1% ammonium acetate or ammonium hydroxide in water. **▼CAUTION:** May cause irritation to skin, eyes, and the respiratory tract; avoid direct contact and inhalation.

3. Electrospray solution for reactive LAESI experiments: reagents, e.g., $\sim 1 \mu\text{M}$ – 1 mM lithium sulfate.
4. Pre-cleaned glass slides (e.g., Thermo Fisher Scientific, Inc., Waltham, MA, USA).
5. Double-sided tape.
6. 1-Methyl-2-pyrrolidinone and an electric heater for the removal of the optical fiber jacket and 1% nitric acid (reagent grade) for the etching of the germanium oxide fiber. ▼CAUTION: Combustible, causes irritation to skin and eyes; and avoid contact with skin and eyes.
7. For plant studies, growth chamber and plant growing protocol (e.g., 14 h photoperiod, 24°C).
8. Cryomicrotome with microtome blades (e.g., Shandon Cryostat, Thermo Fisher Scientific), frozen specimen embedding medium (FSEM, Shandon Cryomatrix, Thermo Fisher Scientific, Inc., Waltham, MA, USA), and liquid N_2 . ▼CAUTION: It causes suffocation when present at amounts sufficient to reduce oxygen concentration below 19.5%. Contact with tissue can cause severe cryogenic burns. Always handle with protective gloves.
9. -80°C freezer (e.g., Revco freezers, Thermo Fisher Scientific, Inc., Waltham, MA, USA).
10. Aluminum foil.

2.2. Mid-IR Ablation on Sample

1. Q-switched mid-IR laser emitting light at $2.94 \mu\text{m}$ wavelength or an optical parametric oscillator tunable in the vicinity of $2.94 \mu\text{m}$ wavelength pumped by a Q-switched Nd:YAG laser (e.g., Oportek, Inc., Carlsbad, CA, USA). ▼CAUTION: Class IV laser; Direct exposure of the eye to the laser beam can cause permanent eye damage. Always wear laser protective eyewear of sufficient optical density at the operating wavelengths.
2. Mirrors for mid-IR light (e.g., gold-coated mirrors, Thorlabs, Newton, NJ, USA).
3. Focusing lens for mid-IR light, e.g., plano-convex CaF_2 or antireflection-coated ZnSe lens (Infrared Optical Products, Farmingdale, NY, USA); or an aspherical lens; or a reflective microscope objective (Newport Corp., Irvine, CA, USA); or a sharpened optical fiber for mid-IR light delivery, e.g., $450 \mu\text{m}$ core germanium oxide-based optical fiber (Infrared Fiber Systems, Silver Spring, MD, USA) with chucks and positioners (e.g., Newport Corp., Irvine, CA, USA) and a three-axis translation stage (e.g., Thorlabs, Inc., Newton, NJ, USA).

4. Thermo- and photosensitive papers for beam alignment and core spot size optimization (e.g., R30C5W, Liquid Crystal Resources L.L.C., Glenview, IL, and multigrade IV, Ilford Imaging Ltd, UK), respectively.
5. Plate holders (e.g., FP02 or FP02, Thorlabs, Inc., Newton, NJ, USA) for sample mounting.
6. Enclosure for the ion source including the laser ablation plume. ▼CAUTION: Ablated particles may become airborne and pose health hazard upon inhalation or contact with skin and eye. Please always be aware of related health risks and take proper measures for protection.
7. For frozen samples Peltier cooling stage (e.g., Ferrotec Corp., Bedford, NH, USA) with heat fan (e.g., Allied Electronics, Inc., Fort Worth, TX, USA), and DC power supply.
8. Optical microscope for measurement of ablation crater dimensions.

2.3. Post-ionization with Charged Droplets

1. Electrospray emitters (e.g., MT320-50-5-5 or FS360-75-30-N-5, New Objective, Inc., Woburn, MA, USA).
2. Metal union, conductive perfluoroelastomer ferrule, fittings, tubing sleeve, fused silica capillary, needle port (e.g., IDEX Health & Sciences, Oak Harbor, WA, USA, or Waters Corp., Milford, MA, USA).
3. Syringe pump (e.g., Harvard Apparatus, Holliston, MA, USA) or an LC solvent-delivery system.
4. For experiments with controlled spaying mode, stainless steel electrode with oscilloscope to perform spray current measurements (e.g., WaveSurfer 452, LeCroy, Chestnut Ridge, NY, USA).
5. High-voltage power supply (e.g., Stanford Research Systems, Inc., Sunnyvale, CA, USA). ▼CAUTION: Electric shock hazard. Please make sure that all electric connections are properly shielded.

2.4. Molecular Imaging and Data Analysis

1. Three-axis translation stage (e.g., Newport Corp., Irvine, CA, USA) with motorized actuators and controller (e.g., with LTA-HS, Newport Corp., Irvine, CA, USA).
2. Mass spectrometer (e.g., Q-TOF Premier, Waters Corp., Milford, MA, USA).
3. Software for correlated positioning of the three-axis translation stage with laser ablation and mass spectrometric data acquisition (written in, e.g., LabView, National Instruments, Austin, TX, USA).

4. Software for data analysis and scientific visualization package for molecular image generation (e.g., Origin, Origin-Lab Corp., Northampton, MA, USA); ImageJ (NIH, available at <http://rsb.info.nih.gov>), Biomap (available at <http://www.maldi-msi.org>).

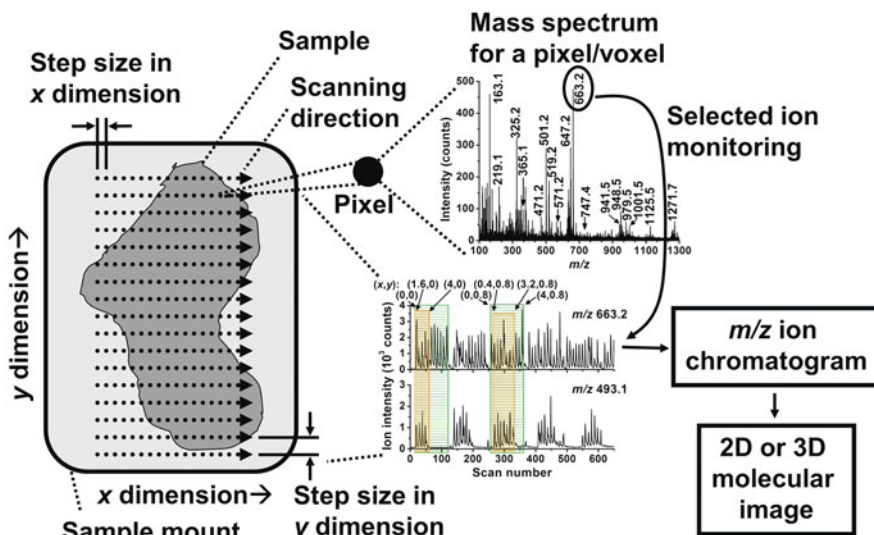
3. Methods

Figure 9.2a shows the workflow of LAESI imaging in an MSI setup. In a 2D imaging experiment, the sample surface is scanned in the focal plane of the mid-infrared laser light, the ablated neutrals and particulate matter are post-ionized with a cloud of charged droplets, and the resulting ions are mass analyzed and recorded. Mass-selected molecular images are reconstructed by correlating the intensity of ion signal for an m/z of interest with the absolute lateral coordinate of analysis for each pixel of the interrogated area (see **Fig. 9.2b** for an *Aphelandra squarrosa* leaf and **Fig. 9.4b,c** for rat brain tissue section). For 3D molecular imaging, the chemical depth profile of the sample is acquired with a selected number of laser pulses delivered at each pixel. The 3D molecular image is represented by a set of 2D images correlated with the absolute depth of analysis (see **Fig. 9.2c**).

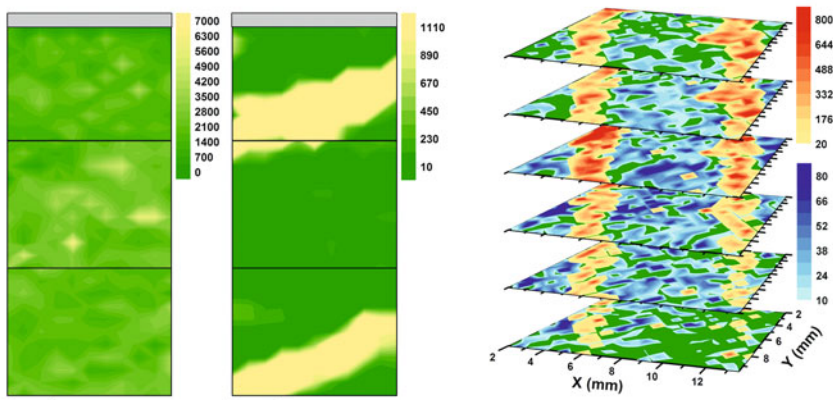
The imaging resolution of LAESI MSI laterally is characterized by the diameter of the ablation crater along with the ablation depth in the third dimension. In regular experiments, lateral step sizes, larger than or equivalent to the diameter of the ablation crater, are applied. The molecular imaging resolution is therefore limited by the divergence of the laser and the properties of the optical focusing component. High-resolution LAESI MSI is also dependent on reliable and effective ion generation at each pixel of the image. Governing factors are the efficiency of the interaction between the electrospray and the laser ablation plumes and the success of entrainment of the resulting droplets and ions into the mass spectrometer. **Figure 9.3a** summarizes the major variables that require optimization for a robust operation. The following section is guidance for setting up a LAESI MSI experiment. For best results, please consider the average ion count for at least three pixels each time adjustment is made to a variable.

3.1. Preparation and Mounting of Tissue

1. Mount sample directly on sample holder with the surface of interest exposed on top and adjust $d_{\text{OR-FP}}$ to ~ 10 mm (see **Fig. 9.3a**). Small clamps and single- and double-sided adhesion tape often enable easy mounting. ▼CAUTION:



(A)



(B)

(C)

Fig. 9.2. (a) Schematics of LAESI MSI in two and three dimensions. Molecular images are obtained by correlating the coordinates of the analyzed pixels with the selected ion abundances. (b) Examples for metabolites with uniform (m/z 663.16 assigned as kaempferol-(diacetyl coumaryl-rhamnoside)) and heterogeneous (m/z 493.10 assigned as methoxy kaempferol glucuronide) lateral distributions in *A. squarrosa* leaves. (Reprinted with permission from (4). Copyright 2008 American Chemical Society.) (c) 3D imaging revealed that kaempferol or luteolin detected at m/z 287.06 (yellow scale) followed the yellow variegation sectors whereas chlorophyll a with m/z 893.54 (blue scale) accumulated in the third and fourth layers of the leaf. (Reprinted with permission from (11). Copyright 2009 American Chemical Society.)

Native water content of sample must be retained for mid-IR light coupling (see Note 4.1.1). (Optional) Evaporative loss of water can be prevented by thaw mounting, whereby the sample is directly frozen onto the sample holder or a glass slide and is kept at low temperatures during imaging (see Fig. 9.4a).

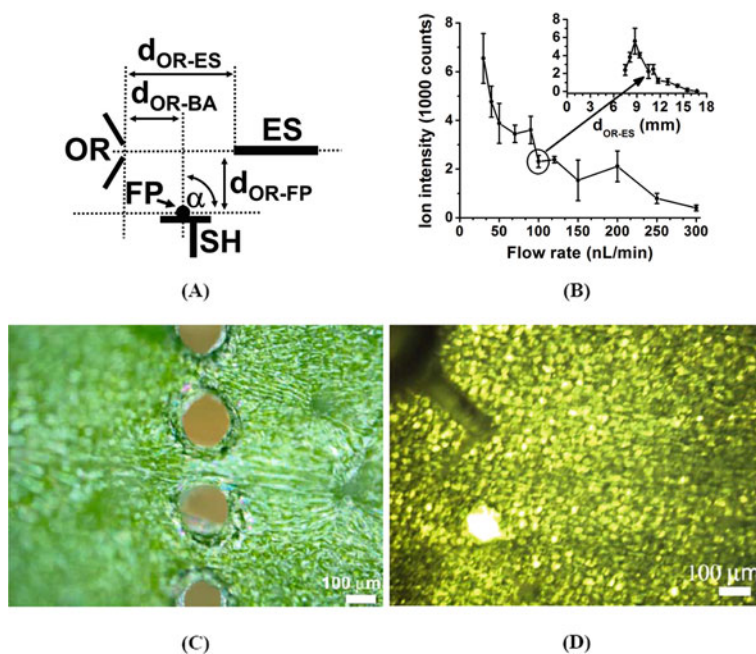


Fig. 9.3. (a) Geometry parameters in a LAESI MSI experiment used to optimize signal-to-noise ratio and lateral and depth resolution of molecular images. The relative position of the electro spray capillary, ES, and the focal point, FP, with respect to the mass spectrometer orifice, OR, and the incidence angle, α , of the laser beam are the essential factors that determine the efficiency of interaction between the ablation plume and the electro spray. (b) The smaller droplets generated by a low flow rate nanospray source (compare the ion intensities at 25 and 300 nL/min) and careful alignment of the ablation plume improved the sensitivity of LAESI MSI. (c) Differential interference contrast microscope image of the adaxial surface of *Arabidopsis thaliana* leaf ablated using a plano-convex ZnSe focusing lens showed tissue removal in an area of $\sim 200 \mu\text{m}$ diameter suggesting a similar lateral resolution for the MSI experiment. (d) Online visualization of tissue sampling with a fiber sharpened to $\sim 50 \mu\text{m}$ (see the top left corner of the image) further improved the lateral resolution by yielding ablation marks of $\sim 100 \mu\text{m}$ in diameter.

2. (Optional) Sectioning may be required for certain tissue types such as animal or human organs. Wrap sample in aluminum foil and dip it into liquid N_2 for ~ 20 s. ▼CAUTION: Improper timing can lead to tissue fracturing. Section tissue into 10–100 μm thick slices with a cryomicrotome at -10 to -20°C . Note that temperature and time requirements might depend on the tissue type. Thaw-mount slices onto microscope slides or directly onto sample holder.
3. (Optional) Store tissues and sections wrapped in aluminum foil at -80°C . This maintains sample integrity for up to a few months. ▼CAUTION: Improper storage conditions can result in postmortem tissue degradation (*see* Note 4.1.2).

3.2. Mid-IR Ablation of Sample

1. For lateral imaging experiment, operate a mid-IR laser at 2.94 μm wavelength and 10 Hz repetition rate. (Optional)

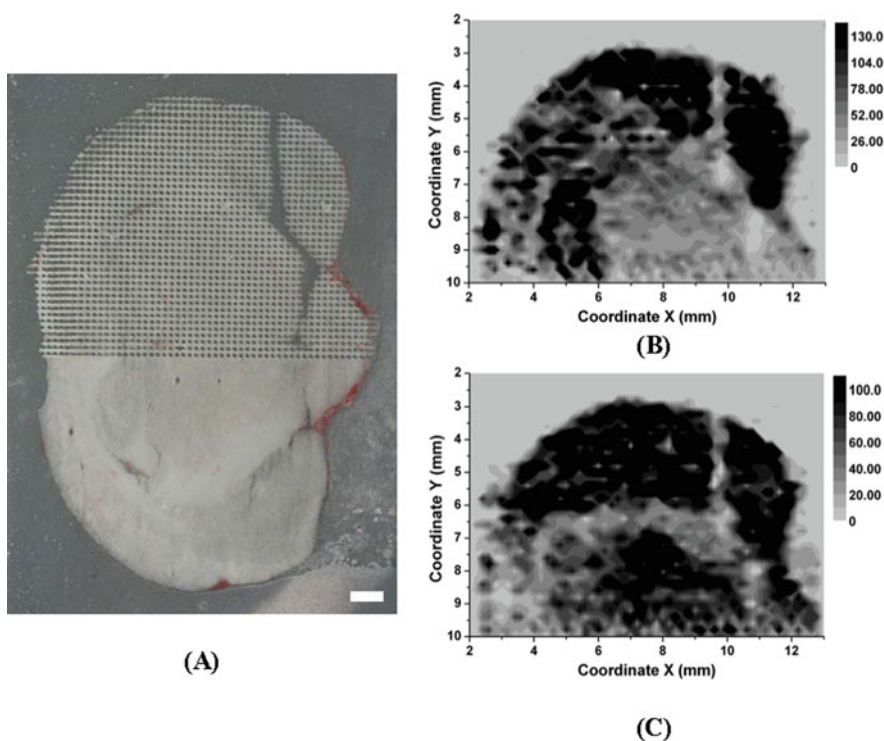


Fig. 9.4. LAESI MSI experiment on ~ 100 μm thick coronal section of a rat (*Rattus norvegicus*) brain. The sample was mounted on a Peltier cooling stage and was kept frozen during imaging to avoid postmortem tissue degradation. (a) The imaged area is shown by an array of ablation marks located 200 μm apart in the x and y directions. Scale bar corresponds to 1 mm. (b) Glycerophosphocholine observed at m/z 258.11 exhibited heterogeneous distribution in the tissue. (c) Glycerophosphocholine (38:6) measured at m/z 806.56 was present throughout the section and appeared especially abundant in the caudate putamen (striatum) and cerebral cortex regions of the brain section.

For samples with low water content (e.g., skin) increase the incident pulse energy. For very low water content samples (such as bone and tooth), tune the laser wavelength to a strong absorption band (*see Note 4.2.1*).

2. Use gold mirrors and a focusing element (e.g., a plano-convex ZnSe lens) to couple the mid-IR laser pulse into the sample at right angle ($\alpha=90^\circ$ in Fig. 9.3a) (*see Note 4.2.2*). Position the focal point below the orifice axis and set $d_{\text{OR-FP}}$ to 5–8 mm (*see Fig. 9.3a*) (*see Note 4.3.3*). ▼CAUTION: Protective enclosure must be used to avoid inhalation of airborne ablated particles.
3. Optimize the position of the focusing element and the pulse energy of the laser beam to achieve tissue removal in desired dimensions – this determines the pixel size (*see Note 4.2.2*). For example, Fig. 9.3c shows that a ZnSe lens allowed the sampling of *Arabidopsis thaliana* with 200 μm diameter ablation mark at 1 mJ/pulse energy. (Optional) Fine focusing can also be achieved by vertical positioning of the

sample holder (*see* SH in **Fig. 9.3a**). Please remain within 5 < $d_{\text{OR-FP}}$ < 30 mm range (*see* **Note 4.3.3**). At distances less than 5 mm the expansion of the ablation plume can destabilize the electrospray (6). Most of the ablated particulate matter does not travel beyond 30 mm due to the drag force in the atmosphere (7).

4. (Optional) Sharpened optical fiber delivery can offer superior lateral resolutions by producing ablation craters with decreased dimensions. For example, **Fig. 9.3d** shows a 100- μm diameter ablation crater. For a GeO_2 -based fiber delivery system, first place ~ 1 cm of both tips of the fiber in boiling 1-methyl-2-pyrrolidinone for ~ 5 min until the polyimide coating is dissolved. **CAUTION:** Work under hood with good ventilation to avoid inhalation of vapor. Wash residues off the glass fiber tip with water and methanol. Cleave both ends for flat surfaces with a diamond scribe and etch one end to desired diameter in 0.1% HNO_3 solution at room temperature (e.g., 50 μm in ~ 15 min). Clean fiber tip with water. Position fiber tip to surface using a three-axis translation stage. **CAUTION:** Etched tip poses sharp object hazard; handle with care.

3.3. Post-ionization with Charged Droplets

1. Position a blunt-tip nanospray emitter (e.g., TaperTipTM with 100 μm inner diameter) in line with the inlet axis of the mass spectrometer and at orifice-to-emitter tip distance, $d_{\text{OR-ES}}$, of ~ 10 mm (*see* **Fig. 9.3a**).
2. Feed 50% methanol solution containing 0.1% acetic acid or 0.1% ammonium acetate for positive and negative ion mode, respectively, through the metal emitter at <300 nl/min. Initiate electrospray by directly applying high voltage to the emitter (*see* **Notes 4.3.1** and **4.3.2**). **Figure 9.3b** reveals that lower flow rates, down to 30 nl/min, give higher kaempferol-(diacetyl coumaryl-rhamnoside) counts when leaf tissues of *A. squarrosa* are studied. The optimum flow rate may be sample dependent as different ablated particulate size distributions may require different electrospray droplet size distributions for sufficient interaction. (Optional) For emitters with nonconductive surface, charge the solution through electrifying a metal union. (Optional) Other organic solvents, such as acetonitrile and isopropanol, may replace methanol. For reactive LAESI imaging, the electrosprayed solution may contain additives (8).
3. While sampling intact sample areas, optimize the spray voltage for LAESI ion yield. (Optional) Follow the temporal behavior of the spray current on a counter electrode with an oscilloscope to determine the flow rate and spray voltage conditions for the cone-jet spraying mode (*see* **Notes 4.3.1**

and 4.3.2). This operating regime, characterized by elevated steady spray current, is reported to be efficient for the post-ionization of ablated particles (6). ▼CAUTION: Avoid electrical breakdown (*see* Note 4.3.3). Sudden rise in the spray current, measured either on the counter electrode or on the orifice of the mass spectrometer, can be an indication of corona discharge. It is usually observed at 3,500–4,000 V for the above-recommended solution, electrosprayed through 100 μm inner diameter emitter.

4. Adjust $d_{\text{OR-BA}}$ (*see* Fig. 9.3a) to optimize horizontally the overlap between the laser plume and the electrospray, thereby improving the LAESI ion yield (*see* Note 4.3.3). Please note that the laser beam, the emitter, and the orifice axis should remain in the same plane with the latter two aligned on the same axis (*see* Note 4.2.2). The inset in Fig. 9.3b shows that an order of magnitude improvement can be achieved in the ion counts by moving the emitter by few millimeters.
5. Optimize $d_{\text{OR-FP}}$ (*see* Fig. 9.3a) while refocusing the lens to retain the pixel size obtained in Section 3.2. The aim of this step is to optimize vertically the overlap between the laser plume and the electrospray, thereby improving the LAESI ion yield. Please note that the laser beam, the emitter, and the orifice axis should remain in the same plane (*see* Note 4.2.2).
6. (Optional) Optimal ion transfer is inherently dependent on the ion source geometry of the mass spectrometer. Fine-tune the position the electrospray emitter perpendicularly to the orifice axis to optimize for ion transfer and repeat Steps 2–6 after each time an adjustment is made.
7. Repeat Steps 2 through 6 for optimum LAESI ion yield.
8. Measure the dimensions of the ablation crater on the sample to be imaged. (Optional) For 3D MSI experiment, perform ablation with individual laser pulses and determine the depth of a voxel.

3.4. LAESI MSI in 2D and 3D

1. Establish software control over the three-axis translation stage and select a gridding algorithm (e.g., adaptive grid, selected region imaging, rectangular grid, spiral pattern, Z scanning) with which to raster the sample surface with selected dwell time at each pixel over the area to be imaged. In our experiments, for example, a LabView program was written in-house to position the sample in a rectangular pattern (e.g., based on left–right scanning shown in Fig. 9.2a) with lateral step sizes in x and y directions equal to or slightly larger than the ablation spot diameter (*see* Fig. 9.4a) (4). Alternatively, molecular imaging can be

performed with lateral step sizes smaller than the diameter of the ablation spot. This approach, also known as oversampling, has been successfully used in combination with classical vacuum and AP IR-MALDI imaging (9, 10). Calculate the total time required for imaging. Wait for START signal to initiate scanning sequence.

2. Operate the mid-IR laser source at a repetition rate sufficient to produce acceptable signal-to-noise ratio in the mass spectrum within the dwell time at each pixel to perform a LAESI 2D MSI experiment. (Optional) For molecular imaging in 3D, use a spectrum acquisition rate higher than the laser source repetition rate to successfully mass analyze the ions generated within a single laser pulse. Wait for START signal to initiate ablation sequence (11).
3. Load the tuning conditions for the ion source of the mass spectrometer and define acquisition parameters (mass range, scan rate, etc.) for the calculated imaging time (*see Note 4.2.2*). Wait for START signal to start the collection of mass spectra.
4. Start the electrospray source at experimental conditions optimized in **Section 3.3**. Please make sure that there is enough electrospray solution in the syringe for the total imaging time.
5. Simultaneously START acquisition of mass spectra, mid-IR ablation, and surface scanning (*see Note 4.3.3*).
6. When imaging has finished, STOP surface scanning, mid-IR lasing, and data acquisition (*see Note 4.3.3*).
7. Turn off spray voltage and stop the flow through the electrospray emitter.

3.5. Data Analysis

1. Correlate absolute coordinates of pixels in 2D or voxels in 3D with the mass spectra to obtain 2D and 3D molecular images (*see Fig. 9.2*).
2. Repeat **Sections 3.1–3.5** to obtain optimal results for a particular experiment. Please review **Section 4** for a list of possible sources of problems, their identification, and prevention during the LAESI MSI experiments.

4. Notes

4.1. Preparation and Mounting of Tissue

1. Evaporative water loss can be a significant source of problems during LAESI MSI experiments. Unsuccessful tissue removal may be an indication of insufficient water content

in the sample. Freeze–thaw mounting and active temperature and/or humidity control during experiments can mitigate these effects.

2. Like in many imaging experiments, improper handling of tissue may result in postmortem degradation. Changing in the chemical composition can yield inconsistent results. Carefully scrutinize sample preparation steps and mounting and storage conditions (*see* **Section 3.1**).

4.2. Mid-IR Ablation of Sample

1. The water content and the mechanical properties, primarily the tensile strength, of the sample are critical factors during mid-IR ablation of samples (12) in LAESI experiments. Although significant changes in these properties can detrimentally affect the imaging results, they are unlikely to occur within a tissue type. These effects would take place, for example, when moving from soft tissue to bone or tooth within a sample. Unsuccessful or incomplete ablation might be an indication of changing water content or tensile strength. Monitor tissue removal at the imaged area and adjust the pulse energy where required.
2. As the LAESI MSI experiments correlate the peak intensity of a particular ion in the mass spectrum with the concentration of the compound at a particular location in the sample (6), it is crucial to ensure that equal amounts of material be ablated from pixel to pixel during the course of the molecular imaging experiment. Significant variations in the diameter and depth of the ablation craters may yield artifacts during the experiment. Likely causes are uneven height of the sample surface, changing angle between the sample holder and the laser beam (α in **Fig. 9.3a**), or temporal variations in the laser pulse stability. Varying water content and tensile strength might further contribute to these effects. Optimize the sample elevation and the relative alignment of the sample holder and the infrared beam axis in **Section 3.2**. Alternatively, adjust the pulse energy to correct for changing ablation dimensions.

4.3. Post-ionization with Charged Droplets

1. Stability of charged droplet generation with the electrospray source is critical for successful ion production with the LAESI source. Sudden changes in the ion or spray current levels usually point to unstable liquid dispersion. Inspect connections and look for material deposition and oxidation on the emitter tip. Clean the emitter tip with the electrospray solvent. Alternatively, replace emitter if required.
2. Liquid filament formation may occur in the negative ion mode and can significantly lower the efficiency of liquid dispersion. In turn, the interception volume between the laser

ablation and the charged droplets is dramatically decreased, causing reduced ion yields. Low LAESI ion yield in the negative ion mode often indicates filament formation. Alter the flow rate and/or the high voltage on the emitter or use a sheath gas.

3. Some ablated particulates may deposit on the electrospray emitter and contaminate the electrospray solvent resulting in regular electrospray ionization. Prolonged presence of ions related to an analyte is often an indication of cross contamination between pixels due to material deposition. Inspect the emitter under optical microscope for significant material deposition. Optimize **Sections 3.2** and **3.3**. for larger $d_{\text{OR-FP}}$ (see **Fig. 9.3a**) and/or increase the $(d_{\text{OR-ES}} - d_{\text{OR-BA}})$ difference by moving the focal point away from the emitter tip. Please note that too large distances may significantly lower the ion yields. Clean emitter tip with the electrospray solution. Replace the emitter if required. Alternatively, use a protective sleeve around the emitter to prevent material deposition on it.

References

1. Cooks, R. G., Ouyang, Z., Takats, Z., Wiseman, J. M. (2006) Ambient mass spectrometry. *Science*, **311**, 1566–1570.
2. Takats, Z., Wiseman, J. M., Gologan, B., Cooks, R. G. (2004) Mass spectrometry sampling under ambient conditions with desorption electrospray ionization. *Science*, **306**, 471–473.
3. Li, Y., Shrestha, B., Vertes, A. (2008) Atmospheric pressure infrared MALDI imaging mass spectrometry for plant metabolomics. *Anal Chem*, **80**, 407–420.
4. Nemes, P., Barton, A. A., Li, Y., Vertes, A. (2008) Ambient molecular imaging and depth profiling of live tissue by infrared laser ablation electrospray ionization mass spectrometry. *Anal Chem*, **80**, 4575–4582.
5. Shelley, J. T., Ray, S. J., Hieftje, G. M. (2008) Laser ablation coupled to a flowing atmospheric pressure afterglow for ambient mass spectral imaging. *Anal Chem*, **80**, 8308–8313.
6. Nemes, P., Vertes, A. (2007) Laser ablation electrospray ionization for atmospheric pressure, *in vivo*, and imaging mass spectrometry. *Anal Chem*, **79**, 8098–8106.
7. Vertes, A., Nemes, P., Shrestha, B., Barton, A. A., Chen, Z. Y., Li, Y. (2008) Molecular imaging by Mid-IR laser ablation mass spectrometry *Appl Phys Mater Sci Process*, **93**, 885–891.
8. Shrestha, B., Nemes, P., Nazarian, J., Hathout, Y., Hoffman, E., Vertes, A. (2010) Direct analysis of lipids and small metabolites in mouse brain tissue by AP IR-MALDI and reactive LAESI mass spectrometry. *Analyst*, **135**, 751–758.
9. Jurchen, J. C., Rubakhin, S. S., Sweedler, J. V. (2005) MALDI-MS imaging of features smaller than the size of the laser beam. *J Am Soc Mass Spectrom*, **16**, 1654–1659.
10. Li, Y., Shrestha, B., Vertes, A. (2007) Atmospheric pressure molecular imaging by infrared MALDI mass spectrometry. *Anal Chem*, **79**, 523–532.
11. Nemes, P., Barton, A. A., Vertes, A. (2009) Three-dimensional imaging of metabolites in tissues under native conditions by laser ablation electrospray ionization mass spectrometry. *Anal Chem*, **81**, 6668–6675.
12. Apitz, I., Vogel, A. (2005) Material ejection in nanosecond Er:YAG laser ablation of water, liver, and skin. *Appl Phys Mater Sci Process*, **81**, 329–338.